J. Biochem. 124, 45-50 (1998)

Lysyl-tRNA Synthetase from *Bacillus stearothermophilus*. Stopped-Flow Kinetic Analysis of Enzyme·Lysyladenylate Formation[1]

Teisuke Takita,* Eriko Akita,† Kuniyo Inouye,* and Ben'ichiro Tonomura[†,2,3]

*Division of Applied Life Sciences, Graduate School of Agriculture, and †Department of Food Science and Technology, Faculty of Agriculture, Kyoto University, Kitashirakawa, Kyoto 606-8502

Received for publication, January 12, 1998

Amino acid activation reaction of the lysyl-tRNA synthetase [L-lysine:tRNA^{Lys} ligase (AMP forming); EC 6.1.1.6] from *Bacillus stearothermophilus* was studied fluorometrically by the stopped-flow method. The addition of L-lysine to the enzyme solution caused quenching of the protein fluorescence and the subsequent addition of ATP restored the quenched fluorescence [Takita *et al.* (1996) *J. Biochem.* 119, 680-689; Takita *et al.* (1997) 121, 244-250]. In the stopped-flow analysis, however, the former fluorescence change (quenching) could not be detected, while the latter change (restoration) was detectable. The L-lysine binding process was suggested to be much faster than the ATP binding process, being completed within the dead-time of the apparatus, *ca.* 3 ms. The hyperbolic dependence of k_{app} on the initial ATP concentration suggested that the ATP binding to the enzyme·L-lysine complex followed a two-step mechanism. Two L-lysine analogues that exhibit the qualitatively similar behavior to L-lysine in the fluorometric titration, L-lysine hydroxamate and L-lysine amide, were examined similarly. The two-step process was also suggested for these analogues, and the forward rate constant in the rate-determining step for L-lysine amide ($221 \pm 7\ s^{-1}$) was significantly larger than those for L-lysine ($45.7 \pm 4.6\ s^{-1}$) and L-lysine hydroxamate ($14.5 \pm 1.7\ s^{-1}$) at pH 8.0, 30°C.

Key words: aminoacyl-tRNA synthetase, fluorescence titration, lysyl-tRNA synthetase, protein fluorescence, stopped-flow analysis.

An aminoacyl-tRNA synthetase (abbreviated as ARS) catalyzes the binding of an amino acid to the cognate tRNA, generally according to the following reaction scheme (*1*).

$$E + AA + ATP \rightleftharpoons E \cdot AA \sim AMP + PP_i \quad (1)$$

$$E \cdot AA \sim AMP + tRNA \rightleftharpoons E + AMP + AA\text{-}tRNA \quad (2)$$

where AA denotes the amino acid; E, ARS; PP_i, inorganic pyrophosphate; and E·AA∼AMP, an ARS· aminoacyladenylate complex. ARSs are divided on the basis of amino acid sequence-alignment into two groups, Class I with "signature sequences" and Class II with "motifs" (*2*). This classification is supported by the initial aminoacylation site of tRNA ribose moiety (*3*) and also by X-ray crystallographic analysis (*4, 5*).

In the previous papers, we reported that the substrate binding to lysyl-tRNA synthetase [EC 6.1.1.6], a Class II enzyme, of *B. stearothermophilus* (abbreviated as *B.s.* LysRS) in the reaction shown in Eq. 1, amino acid activation, followed the sequential ordered mechanism with L-lysine binding first (*6*) and that the binding of L-lysine (abbreviated as L-Lys) to *B.s.* LysRS caused the protein fluorescence to decrease (*6*), but the subsequent addition of ATP restored the decreased fluorescence (*7*). We also reported that L-lysine hydroxamate (abbreviated as L-Lyshxt), produced a stable complex with the enzyme and ATP probably formed an enzyme·lysine hydroxamate-AMP complex (*7*). On the other hand, we could not detect such a complex with L-lysine amide (abbreviated as L-Lysamd).

In this paper, we deal with the transient kinetics of the two processes, the L-Lys binding to *B.s.* LysRS and the ATP binding to the *B.s.* LysRS·L-Lys complex, as examined with the fluorescence stopped-flow method. There have been several reports on the transient kinetics of the amino acid activation reaction. *Escherichia coli* IleRS (*8*) and *E. coli* PheRS (*9*) were investigated by making use of the fluorescence change of a reversibly binding fluorescent probe, 2-*p*-toluidinylnaphthalene-6-sulfonate (abbreviated as TNS), while *B.s.* TyrRS (*10*) and *E. coli* MetRS (*11*) were investigated directly by use of the protein fluores-

[1] This study was supported in part by Grants-in-Aid for Scientific Research from the Ministry of Education, Science, Sports and Culture of Japan, and a Research Grant from the Japan Foundation of Applied Enzymology.

[2] Present address: Research Institute for Biology-Oriented Science and Technology, Kinki University, 930 Nishimitani, Uchita-cho, Naga-gun, Wakayama 649-6493.

[3] To whom correspondence should be addressed.

Abbreviations: ARS, aminoacyl-tRNA synthetase; *B.s.* ARS, ARS from *Bacillus stearothermophilus*; $K_{d,app,A}$, an apparent equilibrium constant for the reaction, E·L-Lys+ATP⇌X; L-Lys, L-lysine; L-Lysamd, L-lysine amide; L-Lyshxt, L-lysine hydroxamate; LysRS, lysyl-tRNA synthetase; TNS, 2-*p*-toluidinylnaphthalene-6-sulfonate. The other aminoacyl-tRNA synthetases are also abbreviated as the three-letter symbol of their specific amino acid followed by RS.

cence. In the case of *B.s.* ValRS (*12*), the binding of a fluorescent ATP analogue, 3′-*O*-anthraniloyl-ATP was investigated. Among them, IleRS, TyrRS, MetRS, and ValRS belong to Class I ARS, and PheRS to Class II. The present report is the first to describe the transient kinetics of the amino acid activation process of a Class II ARS as investigated directly with the change of protein fluorescence as a probe. In addition, we conducted similar kinetic investigations with two lysine analogues, L-Lyshxt and L-Lysamd (*6, 7*), which are strong inhibitors of the reaction shown in Eq. 1.

MATERIALS AND METHODS

Enzyme—*B.s.* LysRS was purified from *B. stearothermophilus* according to the methods described previously (*6*). The enzyme is a homodimer with a subunit molecular weight of 57,700. The enzyme concentration was determined spectrophotometrically with the molar absorption coefficient ε at 280 nm of 71,600 $M^{-1} \cdot cm^{-1}$ at pH 8.0.

Chemicals—L-Lys was the product of Wako Pure Chemical Industries. L-Lyshxt, L-Lysamd, ATP (disodium salt), and β,γ-methylene ATP (sodium salt) were obtained from Sigma Chemical. All other chemicals were of reagent grade.

Stopped-Flow Kinetic Analysis of L-Lys Binding to B.s. LysRS—Before the fluorescence measurement, the purified *B.s.* LysRS was dialyzed against the standard buffer: 100 mM Tris-HCl buffer (pH 8.0) containing 10 mM $MgCl_2$. L-Lys binding to *B.s.* LysRS was studied kinetically by monitoring the fluorescence intensity of the enzyme with a stopped-flow apparatus, Union Giken RA-1300 (gas pressure-driven). The excitation wavelength was 295 nm and the total fluorescence emission was monitored using a cut-off filter with 50% transmission at 310 nm. The enzyme concentration in the reaction mixture was 2.6 μM as the dimer unless otherwise mentioned, while the L-Lys concentration was at least 10 times larger than the enzyme concentration (as dimer). The reaction was carried out in the standard buffer at 30°C. For each reaction condition, more than ten reaction curves were accumulated and averaged by using a kinetic data processor, Union Giken RA-451, to improve the signal-to-noise ratio.

Stopped-Flow Kinetic Analysis of ATP Binding to the Complexes of B.s. LysRS with L-Lys or Its Analogues—The reaction was carried out under the same conditions as described above for L-Lys binding except that the solution containing *B.s.* LysRS and L-Lys was mixed with the solution containing L-Lys and ATP. The enzyme concentration in the reaction mixture was 5.2 μM (as dimer) unless otherwise mentioned. Each solution contained 1 mM L-Lys. On the other hand, the reaction was also carried out by mixing the solution containing only *B.s.* LysRS and the solution containing 2 mM L-Lys and ATP. For the L-Lys analogues, L-Lyshxt and L-Lysamd, the concentration of the analogue in each solution was more than 7-fold larger than its K_d value estimated previously by fluorometric titration in the absence of ATP (*6*).

Fluorometric Titration of Ligand Binding—Fluorometric titration was conducted at 30°C in 100 mM Tris-HCl buffer (pH 8.0) containing 10 mM $MgCl_2$ using a Hitachi 850 fluorescence spectrophotometer. The excitation and emission wavelengths were 295 and 340 nm, respectively. At first, either L-Lys or an analogue (L-Lyshxt or L-Lysamd) was added stepwise to *B.s.* LysRS up to a nearly saturation concentration in the absence of ATP. Then, ATP or its analogue was added stepwise to the solution of a constant first ligand concentration. Titration curves were analyzed by the methods previously described (*6, 7*).

RESULTS

L-Lys Binding to B.s. LysRS—No progress curve of fluorescence was detected with the stopped-flow apparatus for L-Lys binding to *B.s.* LysRS in the range of initial concentration (after mixing) of L-Lys from 30 μM to 1 mM (data not shown). We also examined by the stopped-flow method ATP binding to *B.s.* LysRS in the absence of L-Lys, but no fluorescence progress curve was detected either (data not shown), as expected from the substrate binding order revealed in a previous paper (*6*).

ATP Binding to B.s. LysRS·L-Lys Complex—Figure 1 illustrates a typical progress curve showing the apparent fluorescence increase observed by the stopped-flow method when a solution containing *B.s.* LysRS and 1 mM L-Lys, which had been incubated for 15 min at 30°C, was mixed with a solution containing 1 mM L-Lys and 6 mM ATP. The apparent rate constant k_{app} was calculated from the Guggenheim plot (Fig. 1, inset). The relationship between k_{app} and the initial concentration of ATP showed a hyperbolic saturation curve (Fig. 2). This relationship is consistent with the two-step binding mechanism (*13, 14*) shown in Eq. 3,

$$E \cdot L\text{-}Lys + ATP \underset{k_{-1}}{\overset{k_{+1}}{\rightleftharpoons}} E \cdot L\text{-}Lys \cdot ATP \underset{k_{-2}}{\overset{k_{+2}}{\rightleftharpoons}} X \qquad (3)$$

where X is an isomerized form of the E·L-Lys·ATP complex, and k_{+1}, k_{-1}, k_{+2}, and k_{-2} are the respective rate constants for each step. The first step is fast and in rapid equilibrium, and the second step is experimentally observed. For this mechanism, values of the observed appar-

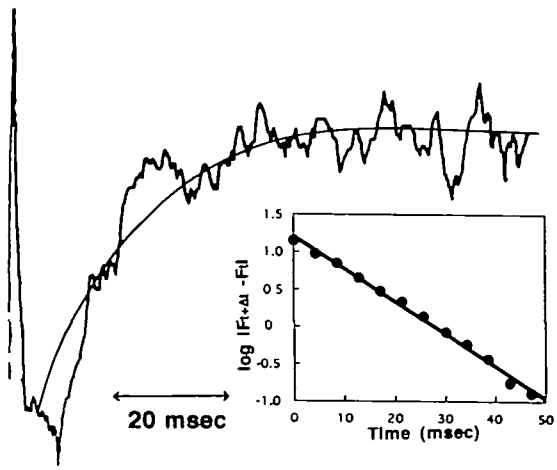

Fig. 1. **Fluorescence stopped-flow trace of the binding of ATP to *B.s.* LysRS·L-Lys complex.** The standard buffer was 100 mM Tris-HCl buffer (pH 8.0) containing 10 mM $MgCl_2$. The reaction was started by mixing the solution containing 5.2 μM *B.s.* LysRS and 1 mM L-Lys and the solution containing 1 mM L-Lys and 6 mM ATP at 30°C. The excitation wavelength was 295 nm and the fluorescence change was monitored by use of a cut-off filter with 50% transmission at 310 nm. The inset shows the Guggenheim plot of the solid curve.

ent first-order rate constant, k_{app}, follow Eq. 4 under the condition that $[ATP]_0 \gg [E]_0$, where $[ATP]_0$ denotes the initial concentration of ATP.

$$k_{app} = k_{-2} + \frac{k_{+2}[ATP]_0}{K_{-1} + [ATP]_0} \quad (4)$$

where K_{-1} is the dissociation constant of E·L-Lys·ATP complex defined as

$$K_{-1} = \frac{[E \cdot L\text{-}Lys][ATP]}{[E \cdot L\text{-}Lys \cdot ATP]} = \frac{k_{-1}}{k_{+1}} \quad (5)$$

The k_{-2} value was evaluated from the intercept of the linear plot of k_{app} against $[ATP]_0$ at low concentrations (Fig. 2, inset). Once the k_{-2} value has been determined, K_{-1} and k_{+2} can be evaluated by the non linear least-squares method (*15*) according to Eq. 4. The values obtained are: $K_{-1} = 523 \pm 136\ \mu M$, $k_{+2} = 45.7 \pm 4.6\ s^{-1}$, and $k_{-2} = 3.1 \pm 2.1\ s^{-1}$ at pH 8.0, 30°C (Table I). The overall dissociation constant of Eq. 3, K_d, was calculated according to Eq. 6.

$$K_d = \frac{[E \cdot L\text{-}Lys][ATP]}{[E \cdot L\text{-}Lys \cdot ATP] + [X]} = \frac{K_{-1}}{1 + K_{+2}} \quad (6)$$

where K_{+2} is the equilibrium constant between E·L-Lys·ATP and X defined as

$$K_{+2} = \frac{[X]}{[E \cdot L\text{-}Lys \cdot ATP]} = \frac{k_{+2}}{k_{-2}} \quad (7)$$

The calculated value of the overall dissociation constant K_d was 33.2 μM. This value is fairly close to the $K_{d,app,A}$ value, the apparent equilibrium constant for the reaction, E·L-Lys + ATP⇌X, 15.5 μM previously estimated by fluorescence titration (7).

When the *B.s.* LysRS solution was mixed with the solution containing 2 mM L-Lys and ATP without preincubation of the enzyme with L-Lys, a similar progress curve of apparent fluorescence increase was also observed (data not shown). Estimated k_{app} values were also plotted against the initial ATP concentration (Fig. 2). The relationship between k_{app} and the initial ATP concentration for the reaction is the same as in the case of the enzyme prein-

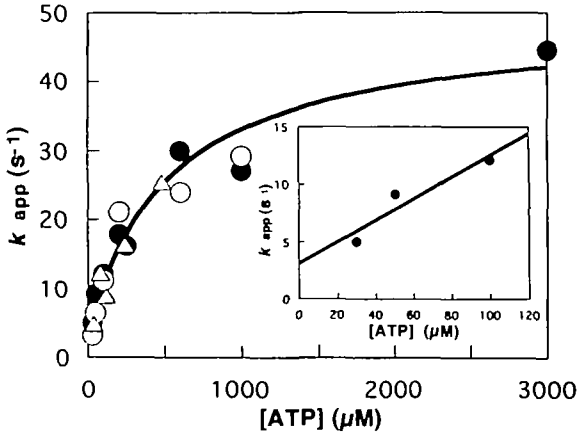

Fig. 2. **ATP concentration dependence of the k_{app} of the ATP binding to *B.s.* LysRS·L-lysine complex.** The standard buffer was 100 mM Tris-HCl buffer (pH 8.0) containing 10 mM $MgCl_2$. The reaction was started at 30°C as follows: ●, (5.2 μM LysRS and 1 mM L-Lys) + (1 mM L-Lys and ATP); ○, (5.2 μM LysRS) + (2 mM L-Lys and ATP); △, (5.2 μM LysRS and 100 μM L-Lys) + (100 μM L-Lys and ATP). The solid curve are the theoretical one drawn according to Eq. 3 with $K_{-1} = 523\ \mu M$, $k_{+2} = 45.7\ s^{-1}$, and $k_{-2} = 3.1\ s^{-1}$. The inset shows the plot at low ATP concentration to determine the k_{-2} value.

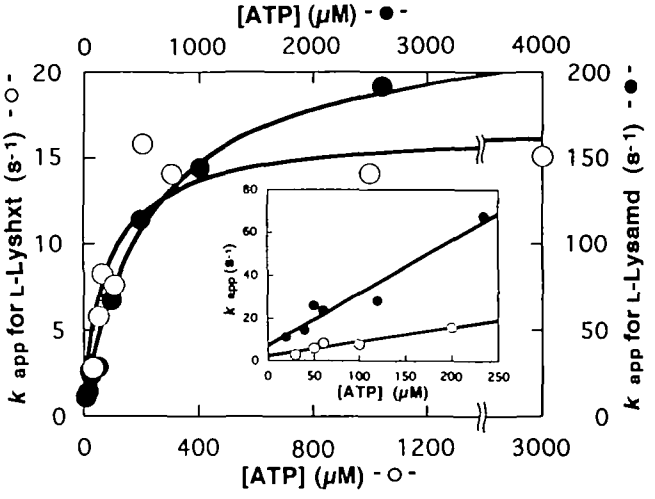

Fig. 3. **ATP concentration dependence of the k_{app} of the ATP binding to *B.s.* LysRS·L-Lys analogue complex.** The standard buffer was 100 mM Tris-HCl buffer (pH 8.0) containing 10 mM $MgCl_2$. The reaction was started at 30°C as follows: ○, (5.2 μM LysRS and 5 mM L-Lyshxt) + (5 mM L-Lyshxt and ATP); ●, (5.2 μM LysRS and 50 mM L-Lysamd) + (50 mM L-Lysamd and ATP). The solid curves are the theoretical ones obtained from the points (○) with $K_{-1} = 99\ \mu M$, $k_{+2} = 14.5\ s^{-1}$, and $k_{-2} = 2.0\ s^{-1}$, and from the points (●) with $K_{-1} = 575\ \mu M$, $k_{+2} = 221\ s^{-1}$, and $k_{-2} = 6.8\ s^{-1}$. The inset shows the plots at low ATP concentration to determine the k_{-2} values.

TABLE I. **Kinetic parameters in the ATP binding process of *B.s.* LysRS.**

LysRS·LA	$\overset{\text{fast}}{\underset{K_{-1}}{\rightleftharpoons}}$ LysRS·LA·ATP	$\overset{\text{slow } k_{+2}}{\underset{k_{-2}}{\rightleftharpoons}}$ X
LysRS·L-Lys	$\overset{\text{ATP}}{\underset{523\ \mu M}{\rightleftharpoons}}$ LysRS·L-Lys·ATP	$\overset{45.7\ (s^{-1})}{\underset{3.1\ (s^{-1})}{\rightleftharpoons}}$ LysRS·L-Lys∼AMP·PP_i
LysRS·L-Lyshxt	$\overset{\text{ATP}}{\underset{99\ \mu M}{\rightleftharpoons}}$ LysRS·L-Lyshxt·ATP	$\overset{14.5\ (s^{-1})}{\underset{2.0\ (s^{-1})}{\rightleftharpoons}}$ LysRS·L-Lyshxt-AMP·PP_i
LysRS·L-Lysamd	$\overset{\text{ATP}}{\underset{575\ \mu M}{\rightleftharpoons}}$ LysRS·L-Lysamd·ATP	$\overset{221\ (s^{-1})}{\underset{6.8\ (s^{-1})}{\rightleftharpoons}}$ LysRS·L-Lysamd·ATP*

LA denotes L-Lys and its analogues (L-Lyshxt and L-Lysamd). The excitation wavelength was 295 nm and the fluorescence change was monitored by the use of a cut-off filter with 50% transmission at 310 nm. The reactions were carried out at 30°C. The standard buffer was 100 mM Tris-HCl buffer (pH 8.0) containing 10 mM $MgCl_2$. In the case of L-Lys, the reaction was started by mixing (*B.s.* LysRS + 1 mM L-Lys) and (1 mM L-Lys + ATP). Other reactions were conducted by replacing 1 mM L-Lys with either 5 mM L-Lyshxt or 50 mM L-Lysamd.

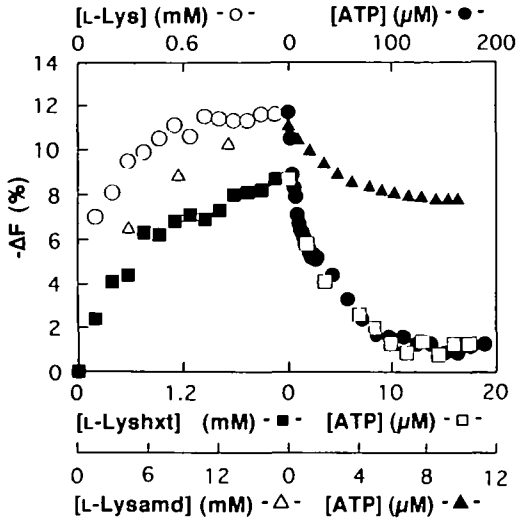

Fig. 4. **Fluorescence titration of *B.s.* LysRS with ATP in the presence of L-Lys, L-Lyshxt, or L-Lysamd.** The reaction mixture consisted of 100 mM Tris-HCl buffer (pH 8.0) containing 10 mM $MgCl_2$ and 4.2 μM LysRS. Three kinds of fluorescence titration (λ_{ex} = 295 nm, λ_{em} = 340 nm) were conducted at 30°C; titration with L-Lys (○) followed by ATP (●) (cited from Ref. 6); titration with L-Lyshxt (■) followed by ATP (□); titration with L-Lysamd (△) followed by ATP (▲).

cubated with L-Lys (Fig. 2). This suggests in turn that the L-Lys binding to *B.s.* LysRS is much faster than the ATP binding to *B.s.* LysRS·L-Lys complex.

ATP Binding to B.s. LysRS·L-Lys Analogue Complex—When the solution containing *B.s.* LysRS and 5 mM L-Lyshxt was mixed with the solution containing 5 mM L-Lyshxt and ATP at pH 8.0, 30°C, the progress curve of fluorescence increase was also observed (data not shown). When the same reaction was carried out by substituting 5 mM L-Lyshxt with 50 mM L-Lysamd, a similar reaction curve was also observed (data not shown). The dependence of k_{app} on the initial ATP concentration (Fig. 3) shows that these reactions can also be considered to follow the two-step binding scheme in both cases. The values obtained at pH 8.0, 30°C when L-Lyshxt was used are: $K_{-1} = 98.9 \pm 39.5$ μM, $k_{+2} = 14.5 \pm 1.7$ s^{-1}, and $k_{-2} = 2.0 \pm 1.3$ s^{-1}; and when L-Lysamd was used: $K_{-1} = 575 \pm 65$ μM, $k_{+2} = 221 \pm 7$ s^{-1}, and $k_{-2} = 6.8 \pm 3.7$ s^{-1} (Table I). The overall dissociation constant, K_d, calculated with Eq. 6 for E·L-Lyshxt + ATP $\rightleftharpoons$ X and E·L-Lysamd + ATP $\rightleftharpoons$ X are 12 and 17 μM, respectively. These values are relatively close to the $K_{d,app,A}$ values obtained when L-Lyshxt and L-Lysamd were used: 3 and 4 μM as previously estimated by fluorescence titration (7).

Fluorescence Titration of B.s. LysRS with ATP and Its Analogue in the Presence of L-Lys or Its Analogues—Figure 4 shows the titration profiles. They are qualitatively similar each other, regardless of the species of L-Lys; however, quantitatively L-Lysamd behaves differently. The titration of *B.s.* LysRS·L-Lys complex with β,γ-methylene ATP showed the same fluorescence restoration as seen with ATP itself (data not shown). This is different from the case of α,β-methylene ATP, which did not exhibit any fluorescence change at all (7).

DISCUSSION

L-Lys Binding to B.s. LysRS—The fact that no progress curve of fluorescence change could be detected in the L-Lys binding process by the stopped-flow analysis suggests either that the process is very fast and is completed within the dead-time of the apparatus (about 3 ms), or that the total L-Lys binding process is slow but composed of two or more steps of which undetectable fast steps involve the fluorescence change but detectable slow steps do not. However, the latter possibility can be excluded because the k_{app} values for ATP binding are similar to each other (Fig. 2) in the cases with and without preincubation of the enzyme with L-Lys. One should note that the binding of L-Lys and ATP to *B.s.* LysRS follows a sequential ordered mechanism with L-Lys binding first (6, 7). Therefore, it is concluded that the L-Lys binding process is much faster than the ATP binding process under our conditions.

There are three previous reports in which the amino acid binding process of ARS was investigated by the stopped-flow method. In each case, the binding order of amino acid and ATP was random. In the case of *E. coli* IleRS (8), where the binding of L-isoleucine to the enzyme at pH 8.0 and 13°C was measured by the use of fluorescence change of TNS, L-isoleucine binding followed a two-step mechanism with $K_{-1} = 93$ μM, $k_{+2} = 125$ s^{-1}, and $k_{-2} = 3$ s^{-1}. However, when the temperature was raised from 13 to 25°C, the L-isoleucine binding became apparently bimolecular (a one-step mechanism). In the case of *B.s.* TyrRS (10), where the L-tyrosine binding to the enzyme at pH 7.78 and 25°C was measured by the use of the protein fluorescence, L-tyrosine binding followed a one-step process with $k_{+1} = 2.4 \times 10^{12}$ $s^{-1} \cdot M^{-1}$ and $k_{-1} = 2.4 \times 10^7$ s^{-1}. In the case of *E. coli* MetRS (11), where the binding of L-methionine to the enzyme at pH 7.6 and 25°C was measured with the protein fluorescence as the probe, the reaction was completed within the dead time (2.5 ms) of the apparatus used. In the case of *E. coli* PheRS (a Class II ARS) (9), it was reported that the rate constant for the binding of TNS to the enzyme (about 200 s^{-1}) did not allow observation of the kinetics for the formation of the enzyme·L-amino acid complex.

ATP Binding to B.s. LysRS—As expected from the results of fluorometric titration (6), no fluorescence progress curve was detected by mixing *B.s.* LysRS with ATP in the absence of L-Lys (data not shown). The binding of ATP to *E. coli* IleRS was investigated by the use of the fluorescence change of TNS (8). In the absence of Mg^{2+}, the binding of ATP to *E. coli* IleRS followed a two-step process with $K_{-1} = 4$ mM, $k_{+2} = 30$ s^{-1}, and $k_{-2} = 4$ s^{-1} at 13°C and pH 8.0, while in the presence of Mg^{2+}, it was drastically accelerated to surpass the capacity of the apparatus. The interaction between *B.s.* ValRS and 3′-*O*-anthraniloyl-ATP, a fluorescent ATP analogue, was also investigated by the fluorescence stopped-flow method (12). The binding of 3′-*O*-anthraniloyl-ATP followed the two-step process with $K_{-1} = 420 \pm 110$ μM, $k_{+2} = 47 \pm 5.1$ s^{-1}, $k_{-2} = 7.1 \pm 1.6$ s^{-1} at pH 7.5, 30°C in the presence of 10 mM $MgCl_2$.

ATP Binding to B.s. LysRS·L-Lys Complex—In the L-Lys activation reaction by *B.s.* LysRS with the protein fluorescence as probe, it appears that the ATP binding process consists of at least two steps as shown in Eq. 3 (Fig. 2 and Table I). In the cases of *E. coli* IleRS (8), *E. coli*

PheRS (*9*), and *E. coli* MetRS (*11*), the amino acid activation reaction measured by the stopped-flow method was analyzed by assuming a random Bi-Uni mechanism in which the association-dissociation equilibria involving AA, ATP, and PP_i were in rapid equilibrium with respect to the rate-determining step of aminoacyl adenylate formation. The same scheme was considered to occur in the case of *B.s.* TyrRS, because on mixing of *B.s.* TyrRS·Tyr∼AMP with PP_i, the fluorescence change observed by the stopped-flow method was concurrent with the formation of ATP analyzed by the quenched-flow method (*10*). From a comparison of the rate constants for the rate-determining step, it turns out that in the cases of *E. coli* IleRS (*8*), PheRS (*9*), and MetRS (*11*), the ratio of k_b/k_f, in which k_b represents the rate constant of the backward reaction at the rate-determining step and k_f, the rate constant of the forward reaction, is close to unity or larger than one. However, in our case with *B.s.* LysRS, the ratio of k_{-2}/k_{+2} (Table I) is less than *ca.* 0.07. This difference may be explained by assuming that X in Eq. 3 represents, E·Lys∼AMP·PP_i $\rightleftharpoons$E·Lys∼AMP+PP_i in rapid equilibrium. With this three-step mechanism, the apparent rate constant would be as follows:

$$k_{app} = \frac{k_f[ATP]}{K_{-1} + [ATP]} + \frac{k_b[PP_i]}{K_{PP_i} + [PP_i]} \quad (8)$$

where

$$K_{PP_i} = \frac{[E \cdot Lys \sim AMP][PP_i]}{[E \cdot Lys \sim AMP \cdot PP_i]}$$

Accordingly, the k_{-2} value estimated in "RESULTS" (Fig. 2) according to Eq. 4, which is based on Eq. 3, would actually be a function of PP_i concentration. Under the conditions of our stopped-flow experiments, $[PP_i] = [E \cdot Lys \sim AMP] < [E]_0 = 5.2\ \mu M$. The value of K_{PP_i} has not been estimated for our system, but it has been reported for other ARS systems to be 100-550 μM (*8, 9, 11*). If such a value is appropriate in our case, the k_b value could be much larger than the present value of k_{-2}, 3.1 s^{-1}. The effects of PP_i concentration on the rate constants are under investigation.

ATP Binding to B.s. LysRS·L-Lys Analogue Complex— We reported that L-Lyshxt was a strong inhibitor in the ATP-PP_i exchange reaction catalyzed by *B.s.* LysRS (*6*) and that its binding to *B.s.* LysRS was significantly enhanced in the presence of ATP (*7*). Under such conditions, a stable *B.s.* LysRS·L-Lyshxt-AMP complex was formed almost irreversibly (*7*). In this complex, a covalent bond was assumed between Lyshxt and AMP by analogy with the complex of *T. thermophilus* SerRS and serinehydroxamate-AMP (*16*). Since the process of L-Lyshxt binding to *B.s.* LysRS could not be detected by the stopped-flow method (data not shown), similarly to L-Lys binding, it is reasonable to consider that the fluorescence change observed by the addition of ATP to a mixture of *B.s.* LysRS and L-Lyshxt was also derived from the ATP binding process, which may include the covalent bond formation between L-Lyshxt and AMP.

L-Lysamd is also a strong inhibitor of the ATP-PP_i exchange reaction catalyzed by *B.s.* LysRS (*6*) and its binding to *B.s.* LysRS is significantly enhanced by the presence of ATP (*7*), similarly to L-Lyshxt. However, L-Lysamd will not form such an aminoacyladenylate intermediate as Lys∼AMP or Lyshxt-AMP because of the absence of the hydroxyl group. Therefore, we consider that the fluorescence change observed upon the addition of ATP to the mixture of *B.s.* LysRS and L-Lysamd is derived from isomerization of the complex, as shown in Table I, where E·L-Lysamd·ATP* is an isomer of E·L-Lysamd·ATP. The k_{+2} value for L-Lysamd is considerably larger than those for L-Lys and L-Lyshxt (Table I). This is consistent with the idea that the observed fluorescence change for L-Lysamd is derived from the isomerization step in the ATP binding process, while the fluorescence changes for L-Lys and L-Lyshxt are derived from the slower covalent bond formation steps of L-Lys∼AMP and L-Lyshxt-AMP.

The inference obtained from the stopped-flow analysis that both the isomerization step and the covalent bond formation step in the ATP binding process cause the protein fluorescence to increase (recover) may allow a clearer interpretation of the results of fluorescence titration (Fig. 4), where the protein fluorescence was decreased by the addition of L-Lys or its analogues (L-Lys, 12.5%; L-Lyshxt, 10.9%; L-Lysamd, 16.6%), but the subsequent ATP addition with a constant first ligand concentration restores the decreased fluorescence to different levels (L-Lys, 91%; L-Lyshxt, 87%; L-Lysamd, 33%). It is suggested that in the cases of L-Lys and L-Lyshxt, the ATP binding process consists of at least four steps: loose ATP binding, isomerization of the complex, covalent bond formation, and the release of PP_i, in which the isomerization step and the covalent bond formation step involve the fluorescence change, and that in the case of L-Lysamd, the process lacks the latter two steps, resulting in the lower recovery of the fluorescence. In the previous paper (*7*), we reported that the addition of α,β-methylene ATP to the E·L-Lys complex did not cause any change in the protein fluorescence. On the other hand, it has been shown in the present study that β,γ-methylene ATP restores the protein fluorescence on the addition to the E·L-Lys complex, in the same manner as ATP does. This suggests a correlation between the fluorescence restoration and ATP hydrolysis to form AMP, and supports, though indirectly, the above conclusion regarding the process of ATP binding to the E·L-Lys complex.

We are grateful to Unitika, Ltd., for their kind supply of *B. stearothermophilus* NCA1503 cells.

REFERENCES

1. Berg, P. (1961) Specificity in protein synthesis. *Annu. Rev. Biochem.* **30**, 293-324
2. Eriani, G., Delarue, M., Poch, O., Gangloff, J., and Moras, D. (1990) Partition of tRNA synthetases into two classes based on mutually exclusive sets of sequence motifs. *Nature* **347**, 203-206
3. Sprintzl, M. and Cramer, F. (1975) Site of aminoacylation of tRNAs from *Escherichia coli* with respect to the 2′- or 3′-hydroxyl group of the terminal adenosine. *Proc. Natl. Acad. Sci. USA* **72**, 3049-3053
4. Cusack, S. (1995) Eleven down and nine to go. *Nature Struct. Biol.* **2**, 824-831
5. Arnez, J.G. and Moras, D. (1997) Structural and functional considerations of the aminoacylation reaction. *Trends Biochem. Sci.* **22**, 159-164
6. Takita, T., Ohkubo, Y., Shima, H., Muto, T., Shimizu, N., Sukata, T., Ito, H., Saito, Y., Inouye, K., Hiromi, K., and Tonomura, B. (1996) Lysyl-tRNA synthetase from *Bacillus stearothermophilus*. Purification, and fluorometric and kinetic

analysis of the binding of substrates, L-lysine and ATP. *J. Biochem.* **119**, 680-689
7. Takita, T., Hashimoto, S., Ohkubo, Y., Muto, T., Shimizu, N., Sukata, T., Inouye, K., Hiromi, K., and Tonomura, B. (1997) Lysyl-tRNA synthetase from *Bacillus stearothermophilus*. Formation and isolation of the enzyme·lysyladenylate complex and its analogue. *J. Biochem.* **121**, 244-250
8. Holler, E. and Calvin, M. (1972) Isoleucyl transfer ribonucleic acid synthetase of *Escherichia coli* B. A rapid kinetic investigation of the L-isoleucine-activating reaction. *Biochemistry* **11**, 3741-3752
9. Bartmann, P., Hanke, T., and Holler, E. (1975) L-Phenylalanine: tRNA ligase of *Escherichia coli* K10. A rapid kinetic investigation of the catalytic reaction. *Biochemistry* **14**, 4777-4786
10. Fersht, A.R., Mulvey, R.S., and Koch, G.L.E. (1975) Ligand binding and enzyme catalysis coupled through subunits in tyrosyl-tRNA synthetase. *Biochemistry* **14**, 13-18
11. Hyafil, F., Jacques, Y., Fayat, G., Fromant, M., Dessen, P., and Blanquet, S. (1976) Methionyl-tRNA synthetase from *Escherichia coli*: Active stoichiometry and stopped-flow analysis of methionyl adenylate formation. *Biochemistry* **15**, 3678-3685
12. Kakitani, M., Tonomura, B., and Hiromi, K. (1989) Static and kinetic studies on binding of a fluorescent analogue of ATP and valyl-tRNA synthetase from *Bacillus stearothermophilus*. *Biochim. Biophys. Acta* **996**, 76-81
13. Czerlinski, G.H. (1966) *Chemical Relaxation, an Introduction to Theory and Application of Stepwise Perturbation*, Marcel Dekker, New York
14. Hiromi, K. (1979) *Kinetics of Fast Enzyme Reactions*, Halsted Press Book, John Wiley & Sons, Kodansha, Tokyo
15. Sakoda, M. and Hiromi, K. (1976) Determination of the best-fit values of kinetic parameters of the Michaelis-Menten equation by the method of least squares with Taylor expansion. *J. Biochem.* **80**, 547-555
16. Belrhali, H., Yaremchuk, A., Tukalo, M., Larsen, K., Berthet-Colominas, C., Leberman, R., Beijer, B., Sproat, B. Als-Nielsen, J., Grübel, G., Legrand, J-F., Lehmann, M., and Cusack, S. (1994) Crystal structure at 2.5 angstrom resolution of seryl-tRNA synthetase complexed with two analogues of seryl adenylate. *Science* **263**, 1432-1436